# End-stacking of copper cationic porphyrins on parallel-stranded guanine quadruplexes

**ARTICLE** *in* JBIC JOURNAL OF BIOLOGICAL INORGANIC CHEMISTRY · DECEMBER 2007

Impact Factor: 2.54 · DOI: 10.1007/s00775-007-0292-0 · Source: PubMed

J Biol Inorg Chem (2007) 12:1235–1249
DOI 10.1007/s00775-007-0292-0

ORIGINAL PAPER

# End-stacking of copper cationic porphyrins on parallel-stranded guanine quadruplexes

**Sarah E. Evans · Miguel A. Mendez · Kevin B. Turner · Loryn R. Keating · Ryan T. Grimes · Sarah Melchoir · Veronika A. Szalai**

Received: 25 June 2007 / Accepted: 12 August 2007 / Published online: 5 September 2007


**Abstract** Nucleic acids that contain multiple sequential guanines assemble into guanine quadruplexes (G-quadruplexes). Drugs that induce or stabilize G-quadruplexes are of interest because of their potential use as therapeutics. Previously, we reported on the interaction of the $Cu^{2+}$ derivative of 5,10,15,20-tetrakis(1-methyl-4-pyridyl)-21*H*, 23*H*-porphine (CuTMpyP4), with the parallel-stranded G-quadruplexes formed by $d(T_4G_nT_4)$ ($n = 4$ or 8) (Keating and Szalai in *Biochemistry* 43:15891–15900, 2004). Here we present further characterization of this system using a series of guanine-rich oligonucleotides: $d(T_4G_nT_4)$ ($n = 5$–10). Absorption titrations of CuTMpyP4 with all $d(T_4G_nG_4)$ quadruplexes produce approximately the same bathochromicity (8.3 ± 2 nm) and hypochromicity (46.2–48.6%) of the porphyrin Soret band. Induced emission spectra of CuTMpyP4 with $d(T_4G_nT_4)_4$ quadruplexes indicate that the porphyrin is protected from solvent. Electrospray ionization Fourier transform ion cyclotron resonance mass spectrometry revealed a maximum porphyrin to quadruplex stoichiometry of 2:1 for the shortest ($n = 4$) and longest ($n = 10$) quadruplexes. Electron paramagnetic resonance spectroscopy shows that bound CuTMpyP4 occupies magnetically noninteracting sites on the quadruplexes. Consistent with our previous model for $d(T_4G_4T_4)$, we propose that two CuTMpyP4 molecules are externally stacked at each end of the run of guanines in all $d(T_4G_nT_4)$ ($n = 4$–10) quadruplexes.

**Keywords** Copper porphyrin · End-stacking · Guanine quartet · Guanine quadruplex · Fourier transform ion cyclotron resonance mass spectrometry and electron paramagnetic resonance spectroscopy

**Abbreviations**

| | |
|---|---|
| CD | Circular dichroism |
| CuTMpyP4 | $Cu^{2+}$ derivative of 5,10,15,20-tetrakis (1-methyl-4-pyridyl)-21*H*,23*H*-porphine |
| EPR | Electron paramagnetic resonance |
| ESI | Electrospray ionization |
| FTICR | Fourier transform ion cyclotron resonance |
| G-quadruplex | Guanine quadruplex |
| $H_2$TMpyP4 | 5,10,15,20-Tetrakis(1-methyl-4-pyridyl)-21*H*,23*H*-porphine |
| MS | Mass spectrometry |
| $Na_2$EDTA | Ethylenediaminetetraacetic acid disodium salt |
| PAGE | Polyacrylamide gel electrophoresis |
| TBE | Tris(hydroxymethyl)aminomethane–borate–ethylenediaminetetraacetic acid |
| Tris | Tris(hydroxymethyl)aminomethane |

## Introduction

Guanine quadruplexes (G-quadruplexes) are nucleic acid structures that have been implicated in biological events

**Electronic supplementary material** The online version of this article (doi:10.1007/s00775-007-0292-0) contains supplementary material, which is available to authorized users.

S. E. Evans · M. A. Mendez · K. B. Turner · L. R. Keating · R. T. Grimes · S. Melchoir · V. A. Szalai (✉)
Department of Chemistry and Biochemistry,
University of Maryland,
Baltimore County,
1000 Hilltop Circle,
Baltimore, MD 21250, USA
e-mail: vszalai@umbc.edu

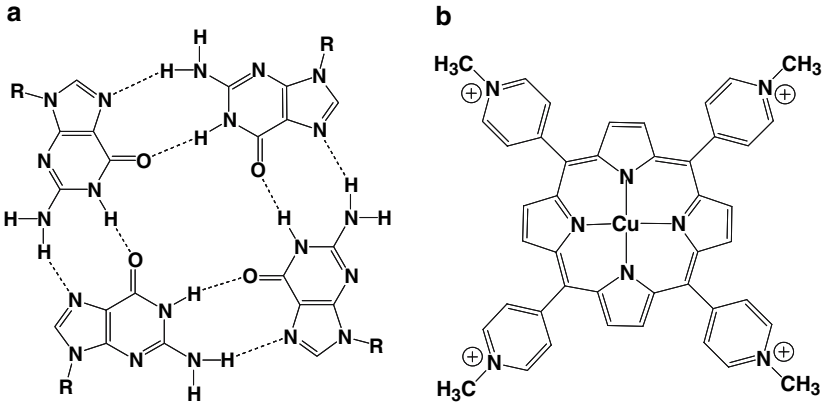


**Fig. 1** **a** Structure of a guanine quartet. **b** Structure of the $Cu^{2+}$ derivative of 5,10,15,20-tetrakis(1-methyl-4-pyridyl)-21*H*,23*H*-porphine (CuTMpyP4)

involving protein–DNA recognition such as replication and transcription [1–8]. The involvement of G-quadruplexes in these processes and their potential to halt propagation of cancerous cells have driven investigation of ligands that stabilize and/or induce formation of G-quadruplexes [9–26].

A DNA (or RNA) G-quadruplex contains multiple guanine quartets, which are planar arrangements of four hydrogen-bonded guanines (Fig. 1a). Intramolecular G-quadruplexes are formed by folding of a single strand of nucleic acid containing several contiguous guanines, whereas intermolecular quadruplexes are generated by association of multiple guanine-rich strands. In addition to their importance in biology, quadruplexes have proven to be attractive tools for biosensor and nanomaterials development [27–37].

Classic duplex DNA-binding ligands, in particular intercalators, interact with G-quadruplexes predominantly via binding at the end of the guanine stack in the quadruplex structure [14, 17, 21–23, 38–41]. We refer to this mode of binding as end-stacking and define it as a binding mode in which a planar ligand stacks on the exterior "face" of a guanine quartet in the quadruplex, even when additional nucleotides flank the guanine stacks. Molecular modeling of intermolecular quadruplexes containing three or four stacks of guanines indicates that end-stacking of ligands is observed because it is energetically unfavorable for short quadruplexes to support ligands positioned between guanines in the guanine stack [11, 42]. The observation of end-stacking on G-quadruplexes is therefore not surprising given that most studies have focused on nucleic acid sequences with three or four guanine quartets [11, 15, 17, 21–24, 38–41, 43]. Read and Neidle [11] have reasonably suggested that G-quadruplexes containing more than four sequential guanine stacks might bind ligands intercalatively between guanines [24, 43]. There is limited characterization of ligand binding to quadruplexes formed by sequences containing more than four contiguous guanines [25, 44–47], making it unclear if there is a quadruplex length at which intercalation between guanines might be observed.

Porphyrins are similar in width to a guanine quartet and have been proposed to bind to G-quadruplexes by end-stacking and intercalation [14, 24, 39, 40, 43, 48–50], depending on the type of quadruplex (intermolecular vs. intramolecular). Significant work has appeared on the porphyrin 5,10,15,20-tetrakis(1-methyl-4-pyridyl)-21*H*,23*H*-porphine ($H_2$TMpyP4) and its derivatives because it stabilizes intramolecular G-quadruplexes and inhibits tumor growth [10, 20]. In contrast to the free-base porphyrin, the interactions of metalloporphyrins with G-quadruplexes have not been investigated intensively [10, 18, 23], even though several metalated derivatives of $H_2$TMpyP4 inhibit the enzyme telomerase, an important target in cancer research [18]. In general, metal complexes have not been exploited as potential G-quadruplex ligands, although recently a square-planar $Ni^{2+}$ complex has been shown to bind selectively to the intramolecular quadruplex formed by human telomeric repeats, thereby inhibiting telomerase [51]. A benefit of metal-containing DNA binders is that they often can be characterized by the same techniques as metal-free ligands, but additionally by methods that probe their unique spectroscopic and/or physical properties.

To further our understanding of the interactions of metalated derivatives of $H_2$TMpyP4 with G-quadruplexes and to probe the possibility that metalloporphyrins might bind between guanines in a G-quadruplex, we have explored the interaction of the $Cu^{2+}$ derivative of $H_2$TMpyP4 (CuTMpyP4) with G-quadruplexes assembled from $d(T_4G_nT_4)$, where $n = 4$–10 (Table 1),[1] using a combination of UV–vis, emission, and electron paramagnetic resonance (EPR) spectroscopies, in addition to high-resolution electrospray ionization (ESI) Fourier transform ion cyclotron resonance (FTICR) mass spectrometry (MS).

[1] Note that throughout the manuscript $[d(T_4G_nT_4)_4]$ corresponds to the tetramolecular quadruplex formed by association of four $d(T_4G_nT_4)$ strands.

**Table 1** Oligonucleotide sequences and extinction coefficients of single-stranded oligonucleotides

| Abbreviation | Sequence | $\varepsilon_{ss}$ ($mM^{-1}$ $cm^{-1}$)[a] |
|---|---|---|
| G4 | TTTTGGGGTTT | 106.4 |
| G5 | TTTTGGGGGTTTT | 116.5 |
| G6 | TTTTGGGGGGTTTT | 126.6 |
| G7 | TTTTGGGGGGGTTTT | 136.7 |
| G8 | TTTTGGGGGGGGTTTT | 146.8 |
| G9 | TTTTGGGGGGGGGTTTT | 156.9 |
| G10 | TTTTGGGGGGGGGGTTTT | 167.0 |

[a] Calculated using the nearest-neighbor approximation; see "Materials and methods" [53]

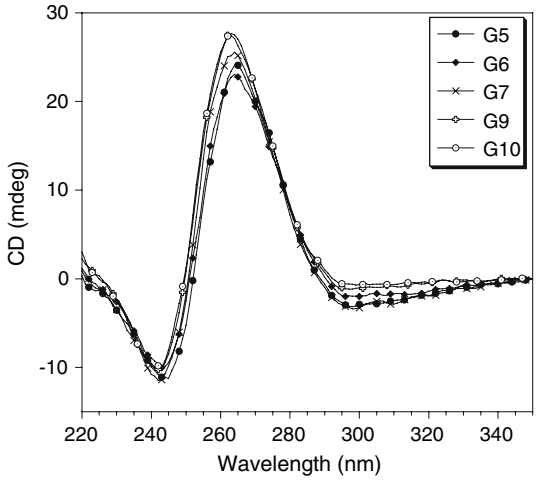


**Fig. 2** Circular dichroism (*CD*) spectra of G5, G6, G7, G9, and G10 (see Table 1) in 10 mM potassium phosphate, 50 mM KCl, pH 7.0. CD spectra were collected at an optical density of approximately 0.8 in the UV region for each oligonucleotide and demonstrate that all of the oligonucleotides give CD spectra characteristic of parallel-stranded guanine quadruplexes

## Materials and methods

### Materials

Water was obtained from a Milli-Q Academic A10 system and had a resistivity of 18.2 $M\Omega^{-1}$ and a total organic content of 34 ppb or less. $H_2$TMpyP4 (tetra-*p*-tosylate salt), piperidine, and dimethylsulfate were purchased from Aldrich (Milwaukee, WI, USA). CuTMpyP4 was synthesized according to the procedure of Pasternack et al. [52] or was purchased as the chloride salt from MidCentury (Chicago, IL, USA). CuTMpyP4 solutions in $H_2O$ were stored in the dark to prevent photodegradation. Potassium chloride was supplied by Acros (Morris Plains, NJ, USA). Solutions of 40% acrylamide–bisacrylamide in a 19:1 ratio were purchased from National Diagnostics (Atlanta, GA, USA). Tetramethylethylenediamine, ammonium persulfate, mercaptoethanol, potassium chloride, and ethylenediaminetetraacetic acid disodium salt ($Na_2$EDTA) were supplied by Acros (Morris Plains, NJ, USA). Tris(hydroxymethyl)aminomethane (Tris), boric acid, urea, monobasic and dibasic potassium phosphate, and glycerol were purchased from Fisher (Pittsburgh, PA, USA). All oligonucleotides were purchased from Midland (Midland, TX, USA). The purity of these oligonucleotides was confirmed by matrix-assisted laser desorption/ionization spectra provided by Midland and by circular dichroism (CD) spectra collected by us (Fig. 2). All oligonucleotides were ethanol-precipitated using ammonium acetate after being resuspended in water. Typically, equal volumes of 5 M ammonium acetate and oligonucleotide in water were combined and vortexed. A volume of 95% ethanol (2.5 times that of the total sample volume) was added to the Eppendorf tube and the solution was placed in a –13 °C freezer for 1 h. The sample was centrifuged at 4 °C for 30 min at 16.1 relative centrifugal force. After removal of the ethanol, the pellet was dried in a speed-vacuum system for 5 min taking care not to overdry the sample. Extinction coefficients for the single-stranded d($T_4G_nT_4$) oligonucleotides were calculated by the nearest-neighbor method (Table 1) [53].

On the basis of CD spectra, all of the d($T_4G_nT_4$) oligonucleotides form G-quadruplexes at room temperature in water, which introduces uncertainty in the oligonucleotide concentrations because the samples are not exclusively single-stranded when the absorbance is measured. Melting experiments to dissociate the quadruplexes were successful only for the shortest oligonucleotides in the series (data not shown), even when 7 M urea was present. Parallel-stranded intermolecular G-quadruplexes containing a $G_4$-tract are extremely stable in solutions containing 5 mM or more $K^+$, with melting temperatures above 95 °C [45, 54–56]. Increasing the number of thymines flanking the guanine run decreases the melting temperature of quadruplexes [57]. For our sequences, the increased number of guanines in G5, G6, G7, G8, G9, and G10 presumably offsets the destabilization of having four thymines on both sides of the stacked guanines. Therefore, we used millimolar concentrations of sodium hydroxide to attempt to disrupt the quadruplexes [44, 58]. This procedure dissociated the quadruplexes, as measured by CD spectroscopy, but the quadruplexes did not reassemble after neutralization (Fig. S1).

Alternatively, attempts were made to determine the concentration of nucleic acid by quantitative phosphate assay [59]. For the G4 quadruplex, the extinction coefficient determined by quantitative phosphate assay is 437.2 ± 16.8 $mM^{-1}$ $cm^{-1}$. This value is only about 3% higher than the value calculated for the G4 quadruplex (425.6 $mM^{-1}$ $cm^{-1}$) by assuming that the quadruplex extinction coefficient is 4 times the nearest-neighbor

single-stranded oligonucleotide extinction coefficient (106.4 $mM^{-1}$ $cm^{-1}$). This result indicates that there is little hypochromicity upon quadruplex formation by G4. Unfortunately, the quantitative phosphate assay did not give reproducible results for the longer quadruplexes, owing to incomplete digestion. The extinction coefficients of all quadruplexes were approximated as 4 times the single-stranded extinction coefficients.

## General radiolabeling and polyacrylamide gel electrophoresis

Oligonucleotides were gel-purified and radiolabeled with [$\gamma$-$^{32}$P]ATP (10 mCi mL–*1*, PerkinElmer Life Sciences, Boston, MA, USA) using T4 polynucleotide kinase (Invitrogen, Carlsbad, CA, USA) as previously described [60]. $^{32}$P-radiolabeled oligonucleotide was added to unlabeled oligonucleotide and the solution was heated to 95 °C for 5 min and allowed to cool slowly to room temperature. CuTMpyP4 was added to samples after annealing. Samples were typically stored overnight at 4 °C. Nondenaturing polyacrylamide gel electrophoresis (PAGE) was performed on 16% polyacrylamide gels containing 20 mM KCl. Gel electrophoresis was performed at 4 °C for 4–6 h at 300–350 V. The electrophoresis running buffer was 0.5× Tris–borate–ethylenediaminetetraacetic acid (TBE) with 20 mM KCl. The 0.5× TBE was prepared from a 10× TBE stock containing 0.89 M Tris, 20 mM $Na_2EDTA$, and 0.89 M boric acid, pH 8.3. All gels were wrapped and placed on a phosphor screen, exposed for 1 h for quantification of band intensities, scanned on an Amersham Biosciences Typhoon 9200 instrument, and analyzed using ImageQuaNT$^{TM}$ software.

## Circular dichroism spectroscopy

CD spectroscopy was performed at room temperature using a JASCO J-715 spectropolarimeter coupled to a Dell Optiplex GX110 personal computer for data collection. A quartz cuvette with a 0.3- or 1-cm pathlength was used for all CD experiments. Solutions for CD analysis in 10 mM potassium phosphate with 50 mM KCl, pH 7.0 contained G5, G6, G7, G9, and G10 at a matched optical density of approximately 0.8 for all samples. Each spectrum collected was an average of three scans. A spectrum of the corresponding buffer was collected and its spectrum was subtracted from the spectra of the samples.

An induced CD spectrum of CuTMpyP4 collected under conditions of excess quadruplex was collected for solutions containing 42 μM G6 strand and 3.46 μM CuTMpyP4. Sixteen scans were collected and averaged. The subtracted background spectrum was the spectrum of the corresponding buffer containing 3.46 μM CuTMpyP4.

## UV absorption titrations

Potassium was added from a pH 7.0 stock solution of 1 mM potassium phosphate, 5 mM KCl to water solutions of oligonucleotides. The absorbance at 295 nm was monitored as a function of $K^+$ addition. The concentrations of the oligonucleotides were 4 or 24 μM strand. Two oligonucleotide concentrations were used to confirm that the changes observed at 295 nm were concentration-independent. The higher concentration also was chosen to ensure reliable quantitation of the absorbance changes.

## Visible absorption titrations

Room-temperature absorption spectra were collected using the methods previously reported [61] except that a six-cell sample holder was used in a JASCO V-560 UV–vis double-beam spectrophotometer. Data were analyzed as described in Keating and Szalai [61]. The initial concentration of free CuTMpyP4 was determined from the absorbance at 425 nm using the published extinction coefficient of $2.31 \times 10^5$ $M^{-1}$ $cm^{-1}$ [52]. At least three titrations were performed for G5, G6, G7, G8, G9, and G10 to give average extinction coefficients and hypochromicities for bound CuTMpyP4.

## Continuous-variation analysis

Stock solutions of CuTMpyP4 and quadruplex were prepared in 10 mM potassium phosphate and 50 mM KCl, pH 7.1. The concentration of quadruplex was determined using an extinction coefficient that was 4 times the single-stranded oligonucleotide extinction coefficient, which had been calculated by the nearest-neighbor approximation. Two types of solutions were used for the experiments: one with varying mole fractions of CuTMpyP4 and oligonucleotide in 0.1 mole fraction increments and one with varying concentrations of CuTMpyP4. Solutions containing porphyrin and oligonucleotide contained a constant total (CuTMpyP4 plus quadruplex) concentration of 1 or 3 μM. To obtain mole fractions in 0.05 increments, the solutions in 0.1 mole fraction increments were combined.

Alternatively, a solution of CuTMpyP4 was titrated into an equimolar quadruplex sample solution and reference (buffer) solution. This approach keeps the total concentrations of reactants constant when the concentrations of the starting reactant solutions are matched, but varies the

CuTMpyP4 to quadruplex ratio [62]. During the course of the titration, the solution volume is decreased in order to continue making additions. Data are collected immediately before and after removal of excess volume to verify that the absorption is identical. In these experiments, the concentration of quadruplex in the sample was calculated on the basis of a quadruplex extinction coefficient that was assumed to be 4 times that of the single-stranded oligonucleotide extinction coefficient [i.e., 546.8 $mM^{-1}$ $cm^{-1}$ in terms of quadruplexes for $(G7)_4$].

In both experimental protocols, absorbance difference spectra were collected and analyzed as described previously [61] except that methacrylate cuvettes with a 1-cm pathlength were used to avoid adsorption of the porphyrin on the quartz surface. The wavelengths used to calculate the absorbance difference were 438 and 417 nm.

### Emission spectroscopy

Emission spectra were collected at room temperature using a Jobin-Yvon-Spex Fluorolog-3 fluorimeter as described previously [61] except that the photomultiplier tube correction file supplied by the manufacturer was applied to the spectra. Solutions contained 5 μM CuTMpyP4 with approximately 5 μM oligonucleotide strand. The excitation wavelength was 434 nm, which corresponds to the absorption maximum for fully bound porphyrin.

### Electron paramagnetic resonance spectroscopy

EPR spectra were collected using a Bruker EMX 6/1 X-band spectrometer equipped with an Oxford Instruments ESR900 liquid He cryostat as outlined previously [61]. Samples were prepared by combining stock solutions of CuTMpyP4 and oligonucleotide in water in the appropriate amounts to give desired final concentrations of 50 μM CuTMpyP4 and 25 μM quadruplex. The water was removed and the sample was resuspended in 200 μL of 10 mM potassium phosphate with 50 mM KCl at pH 7.0 containing glycerol (50% v/v).

### Mass spectrometry

Preformed quadruplexes of G4 and G10 in 10 mM potassium phosphate, 50 mM KCl at pH 7 were ethanol-precipitated in 10 M ammonium acetate [63, 64]. The resulting precipitates were redissolved in ammonium acetate (100 mM, pH 7.5) and were extensively desalted by ultrafiltration on Centricon YM-3 devices (Millipore, Bedford, MA, USA) using ammonium acetate (100 mM, pH 7.5). A multiplexed binding assay was performed by mixing equimolar concentrations of preformed $(G4)_4$ and $(G10)_4$ in 100 mM ammonium acetate (pH 7.5), resulting in approximate final 5 μM concentrations of each quadruplex. A stock solution of 100 μM CuTMpyP4 was added in appropriate volumes to give 10 or 50 μM final concentrations, corresponding to an approximately equimolar or fivefold excess of porphyrin over quadruplex. Each sample was incubated at room temperature for 15 min to ensure that a binding equilibrium was established in solution before ESI–FTICR–MS analysis. We have determined previously that binding is complete in less than 10 min [61] and control experiments performed with longer incubation times provided no detectable difference in binding.

Immediately prior to analysis, analyte solutions were mixed with a 10% volume of 2-propanol to reduce the surface tension and facilitate the achievement of stable electrospray [65]. This addition did not have any adverse effect on the state of association of the noncovalent complexes investigated in this study [66], but the dilution factor was taken into account in subsequent calculations. Approximately 3 μL of each sample was loaded into an uncoated quartz nano-ESI needle (New Objective, Woburn, MA, USA). A Pt wire was inserted from the back to carry the necessary voltage (750–1,000 V). Each analysis was performed with a Bruker Daltonics (Billerica, MA, USA) Apex III FTMS system equipped with a 7-T actively shielded superconducting magnet and an Apollo thermally assisted electrospray source. The desolvation interface was set to a temperature of 170 °C. Spectra were acquired in negative ion mode and processed using XMASS 6.0.2 (Bruker Daltonics). A resolving power of approximately 150,000 was typically obtained in broadband mode. An accuracy of approximately 10 ppm or better was achieved using a three-point external calibration of cesium iodide.

## Results

### Circular dichroism

CD spectra of G5, G6, G7, G8, G9, and G10 display clean CD spectra with a positive CD band near 260 nm and a negative CD band near 240 nm characteristic of parallel-stranded G-quadruplexes (Fig. 2) [67]. Under conditions of excess quadruplex, a small, negative induced CD spectrum was observed for the porphyrin at the Soret wavelength of bound porphyrin (435 nm) determined from the absorption titrations (Fig. S2).

## Absorption titrations

The 295-nm absorption of G4, G6, and G10 oligonucleotides in water decreases by about 12% upon the addition of $K^+$ ions (Table S1). On the basis of CD spectra, this decrease corresponds to quadruplex formation (data not shown). At the end of the titration, the total concentration of $K^+$ was no more than 0.51 mM. These results indicate that the quadruplex is the major species present in experiments performed in 10 mM potassium phosphate buffer at pH 7.0 containing 50 mM KCl.

Absorption spectra from the titrations of CuTMpyP4 with G5, G6, G7, G8, G9, and G10 are shown in Fig. 3 and representative complete titration data are given in Fig. S3. All of the redshifts and hypochromicities of the CuTMpyP4 Soret band are in the same range, regardless of the number of guanines in the oligonucleotide (Table 2). Binding curves for CuTMpyP4 with the oligonucleotides plateau at approximately the same concentration of added oligonucleotide (Fig. S4). These binding curves cannot be used to determine the number of CuTMpyP4 molecules bound per mole of quadruplex because the lattice was titrated into a solution of the ligand [68]. Binding constants and stoichiometry can be determined from Scatchard plots, but only confidently under conditions where the plots are linear or the titration is complete [69]. The curvature in our Scatchard plots (Fig. S5) indicates the existence of more than one type of binding site, ligand–ligand interactions, or neighbor-exclusion effects [70], which means they cannot be used directly to obtain binding stoichiometry or affinity.

## High-resolution mass-spectrometric analysis

The stoichiometry of the different CuTMpyP4–quadruplex complexes formed in solution was determined directly by ESI–MS [71, 72]. Owing to its very soft character, this ionization technique is routinely employed for the characterization of nucleic acid substrates and ligands [73–75]. The ability to obtain accurate snapshots of these complexes without disrupting their binding equilibria is substantiated by the direct determination of their relative [76–81] and absolute [66, 80, 82–85] binding affinities in solution. For this reason, ESI–MS has been extensively utilized to explore the binding interactions of quadruplexes with small molecule ligands [47, 84, 86–90]. Here, we used ESI in combination with FTICR–MS [91, 92] to determine the stoichiometry of CuTMpyP4 binding to G4 and G10 quadruplexes.

The ESI–FTICR mass spectra obtained from preformed $(G4)_4$ and $(G10)_4$ substrates in the presence of potassium (see "Materials and methods") provided the expected signals corresponding to intact quadruplexes (four

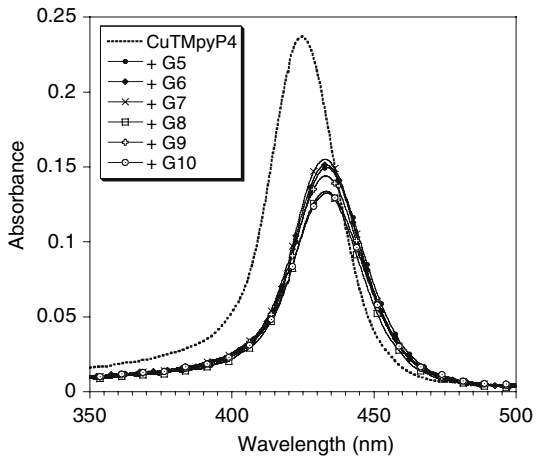


**Fig. 3** Absorption spectra of 1 μM CuTMpyP4 with $d(T_4G_nT_4)$ oligonucleotides in 10 mM potassium phosphate, 50 mM KCl, pH 7.1. Spectra with G5, G6, G7, G8, G9, and G10 are the titration endpoints

oligonucleotide strands plus the specifically bound $K^+$ ions), as well as those corresponding to the initial single-stranded components (Fig. 4, spectrum a). It is important to note that the tuning of the ESI source was adjusted to the mildest desolvation conditions that will prevent observation of nonspecific ammonium or water adducts [93]. Furthermore, nondenaturing PAGE analysis of the same samples showed bands corresponding to the single-stranded components (Fig. S6), thus confirming that these species are present in the samples and are not the product of gas-phase dissociation in the ESI interface.

In the presence of an equimolar amount of CuTMpyP4, complexes with one and two ligand units per quadruplex were readily recognized by ESI–FTICR–MS for both quadruplexes (Fig. 4, spectrum b). When a fivefold excess of CuTMpyP4 was incubated with the preformed

**Table 2** Absorption titration parameters for the $Cu^{2+}$ derivative of 5,10,15,20-tetrakis(1-methyl-4-pyridyl)-21*H*,23*H*-porphine (CuTMpyP4) with oligonucleotides

| Oligonucleotide | $\varepsilon_{bound} \times 10^{-5}$ ($M^{-1}$ $cm^{-1}$) | Soret band shift (nm) | Hypochromicity (%)[a] |
|---|---|---|---|
| $(G5)_4$ | 1.20 ± 0.02 | 8.4 ± 0.3 | 47.9 ± 0.6 |
| $(G6)_4$ | 1.23 ± 0.02 | 8.4 ± 0.2 | 46.6 ± 0.7 |
| $(G7)_4$ | 1.25 ± 0.04 | 8.0 ± 0.2 | 46.0 ± 1.6 |
| $(G8)_4$ | 1.21 ± 0.06 | 8.4 ± 0.2 | 47.6 ± 0.3 |
| $(G9)_4$ | 1.21 ± 0.03 | 8.2 ± 0.2 | 47.7 ± 1.3 |
| $(G10)_4$ | 1.19 ± 0.02 | 8.5 ± 0.3 | 48.6 ± 1.0 |

The errors are standard deviations calculated from at least three titrations

[a] Soret band hypochromicity calculated using the average extinction coefficient for bound CuTMpyP4 derived from multiple titrations; see "Materials and methods"

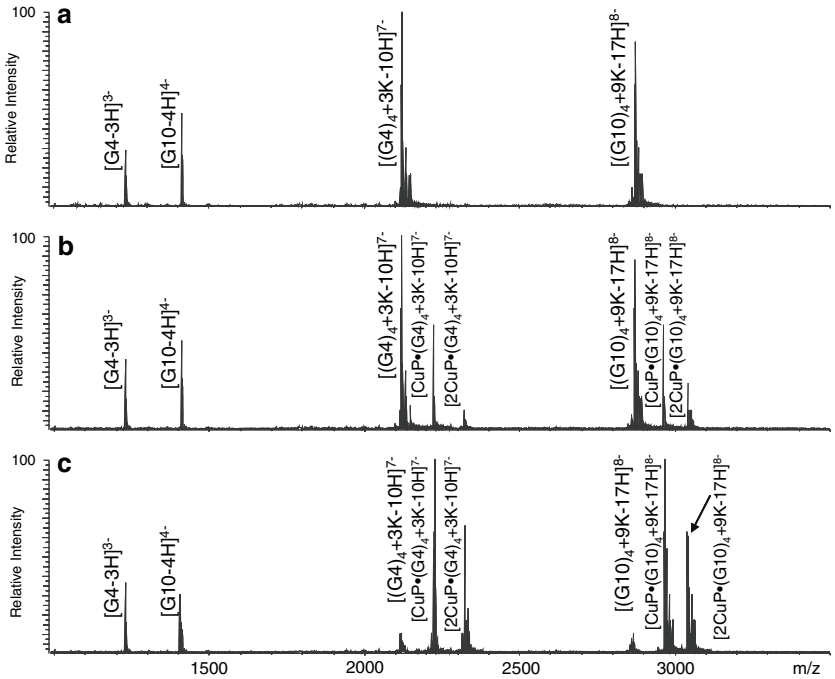


**Fig. 4** Electrospray ionization Fourier transform mass spectrometry data of $(G4)_4$ and $(G10)_4$ with and without CuTMpyP4. **a** Approximately 5.0 μM G4 and 5.0 μM G10 in 100 mM ammonium acetate (pH 7.5) and 10% volume 2-propanol. In the absence of ligand, both single-stranded and quadruplex forms were observed for both species. The single-stranded species of G4 and G10 provided experimental masses of 3,686.24 and 5,660.88 Da, respectively (3,686.62 and 5,660.93 Da calculated from the sequence). The quadruplex species of G4 $[(G4)_4 + 3K^+]$ and G10 $[(G10)_4 + 9K^+]$ provided experimental masses of 14,863.21 and 22,994.59 Da, respectively (14,863.47 and 22,994.72 Da calculated). **b** Approximately 5.0 μM $(G4)_4$ and 5.0 μM $(G10)_4$ in the presence of an equimolar amount of CuTMpyP4 (10 μM). The 1:1 complex $[CuTMpyP4{\cdot}(G4)_4 + 3K^+]$ provided a mass of 15,555.82 Da (15,555.77 Da calculated) and the 1:1 complex $[CuTMpyP4{\cdot}(G10)_4 + 9K^+]$ provided a mass of 23,687.11 Da (23,687.02 Da calculated). **c** Approximately 5.0 μM G4 and G10 with fivefold molar excess CuTMpyP4. A stoichiometry of 2 was observed (e.g., $[2CuTMpyP4{\cdot}(G4)_4 + 3K^+]$ or $[2CuTMpyP4{\cdot}(G10)_4 + 9K^+]$), resulting in increments of 692.30 Da. No binding of the CuTMpyP4 to the single-stranded oligonucleotides was observed and CuTMpyP4 to quadruplex stoichiometries larger than 2 were not detected. *CuP* CuTMpyP4

quadruplexes, an increased abundance of the 2:1 complex was observed in solution, but no higher-order binding was detected (Fig. 4, spectrum c). An attempt to induce further CuTMpyP4 binding by a tenfold increase in the ligand concentration failed to create higher-order assemblies, but resulted only in significant deterioration of the overall spectral quality owing to signal suppression (data not shown). Finally, no further binding was observed even after the desolvation conditions were appropriately adjusted to enable the detection of nonspecific ammonium adducts. Therefore, we conclude that the direct ESI–FTICR–MS determinations of the CuTMpyP4–quadruplex complexes provided a very accurate representation of the solution equilibria within the range of concentrations explored by these experiments.

## Continuous-variation analysis

We also determined the CuTMpyP4 binding stoichiometry using the method of continuous-variation analysis [94–96]. These results indicated that the porphyrin to quadruplex stoichiometry increased from 2:1 for $(G5)_4$ to much higher stoichiometries for the longer quadruplexes (Fig. S7). The binding stoichiometries range from approximately three CuTMpyP4 molecules per $(G6)_4$ to approximately six CuTMpyP4 molecules per $(G10)_4$. The increasing ligand stoichiometry as a function of increased quadruplex length was unexpected on the basis of the MS results. In addition, other spectroscopic characterizations of CuTMpyP4 binding to the $d(T_4G_nT_4)$ quadruplexes are almost identical irrespective of quadruplex length.

To explore the apparent discrepancy between the MS and the continuous-variation analyses, continuous-variation analysis was performed with $(G7)_4$ under conditions where the quadruplex extinction coefficient was varied (Fig. 5b, c). We picked two different quadruplex extinction coefficients for $(G7)_4$: 360.9 $mM^{-1}$ $cm^{-1}$ (34% decreased) or 136.7 $mM^{-1}$ $cm^{-1}$ (75% reduced). The data in Fig. 5 show that the quadruplex extinction coefficient has a dramatic effect on continuous variation analysis data. When

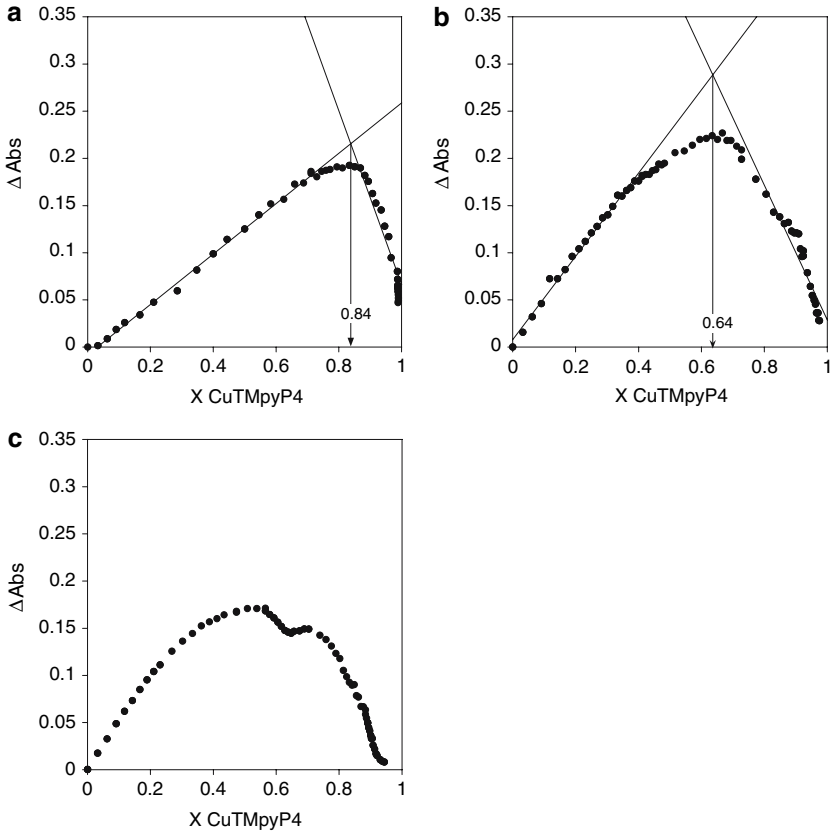


**Fig. 5** Job plots resulting from the method of continuous-variation analysis for 3 μM CuTMpyP4 with $(G7)_4$. **a** Data collected with 3 μM $(G7)_4$, calculated assuming an extinction coefficient of 546.8 $mM^{-1}$ $cm^{-1}$ for the quadruplex. **b**, **c** Job plots for 3 μM $(G7)_4$, calculated assuming 34 or 75% hypochromicity of the quadruplex, respectively. The titration method described in "Materials and methods" was used to obtain data. For all plots, the absorbance difference ($\Delta Abs$) was measured in difference spectra at 438 and 417 nm

360.9 $mM^{-1}$ $cm^{-1}$ was assumed, the binding stoichiometry was 1.8 CuTMpyP4 molecules per quadruplex, in good agreement with the MS data. Further decreasing the extinction coefficient to 136.7 $mM^{-1}$ $cm^{-1}$ gave a Job plot with multiple maxima.

Two other continuous-variation experiments were performed to rule out possible reasons for the stoichiometry differences between the MS and continuous-variation experiments. First, continuous variation was conducted in the same 100 mM ammonium acetate buffer used for the MS experiments. Next, the potassium phosphate buffer concentration was increased to 1 M (Fig. S8). These Job plots are superimposable on the Job plot determined for the G10 quadruplex in 10 mM potassium phosphate, 50 mM KCl buffer. Thus, electrostatic interactions (as probed by the increased salt concentration) and buffer type do not explain the variability in CuTMpyP4 to quadruplex stoichiometry as a function of quadruplex length observed in continuous-variation experiments.

## Emission spectra

Solutions of four CuTMpyP4 per $[d(T_4G_nT_4)_4]$ quadruplex display emission spectra with an emission maximum at 823 ± 1.6 nm (Fig. 6). After correction, these spectra are less broad than those published for CuTMpyP4 intercalated into guanine-rich duplex DNA [97].

## Electron paramagnetic resonance spectroscopy

Low-temperature spectra of CuTMpyP4 show increased resolution in the high-field region of the spectrum in the presence of oligonucleotide (Fig. 7). The main features in EPR spectra of monomeric $Cu^{2+}$ porphyrins arise from hyperfine coupling between the unpaired electron on $Cu^{2+}$ and the $^{63,65}Cu$ $I = 3/2$ nucleus and from superhyperfine coupling with $^{14}N$ ($I = 1$) atoms of the porphyrin [98, 99]. The spectra of CuTMpyP4 with the G-quadruplexes in Fig. 7 have $A_{\|}$ values of 203 ± 4 G and $g_{\|}$ of approximately 2.20. These EPR parameters are very similar to those reported for CuTMpyP4 bound to long strands of random-sequence DNA [100–102]. The average nitrogen hyperfine coupling constant ($A_N$) is 15.8 ± 0.62 G for CuTMpyP4 in buffer and 16.4 ± 0.20 G for CuTMpyP4 bound to any of the $d(T_4G_nT_4)$ quadruplexes (Fig. 7b) [100]. It is significant that the spectra show no evidence of magnetically interacting $Cu^{2+}$ ions (for examples of such spectra, see [98, 103, 104]), a spectral signature that would be expected if the CuTMpyP4 molecules were stacked together on the same side of the quartet stacks.

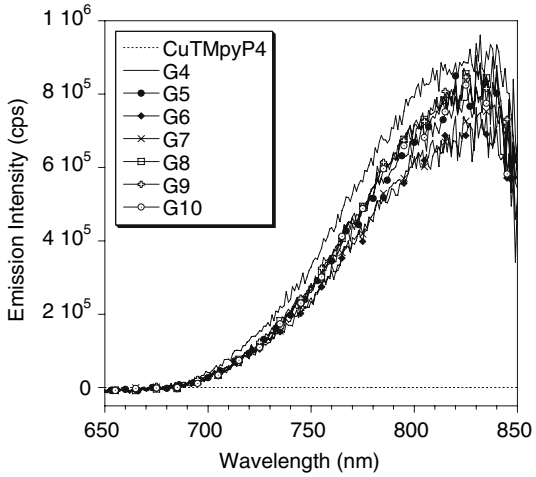


**Fig. 6** Emission spectra ($\lambda_{ex}$ = 434 nm) of 4:1 CuTMpyP4 to G5, G6, G7, G8, G9, or G10 quadruplex. All solutions contained 10 mM potassium phosphate, 50 mM KCl, pH 7.1

## Discussion

The oligonucleotides used in our study form intermolecular parallel-stranded G-quadruplexes in 10 mM potassium phosphate and 50 mM KCl [13, 22, 105–107]. We evaluated quadruplex formation using several methods. First, the absorbance at 295 nm was monitored as a function of $K^+$ addition to solutions of G4, G6, and G10 in water. All of the $d(T_4G_nT_4)$ oligonucleotides form quadruplexes in water on the basis of CD spectra; however, we wanted to establish the $K^+$ concentration required for maximal quadruplex formation by these oligonucleotides. G4, G6, and G10 all showed a 12% decrease in the 295-nm absorbance as the $K^+$ concentration increased, with a concomitant increase in the signature CD spectrum for a parallel-stranded quadruplex. A decrease in the 295-nm absorbance has been associated with quadruplex dissociation [45, 108]. Our results corroborate the importance of the 295-nm absorbance in assessing quadruplex structure; however, they also indicate that changes at 295 nm must be interpreted carefully [108]. For example, thermal difference spectra of the intramolecular quadruplex formed by 5′-AGGG(TTAGGG)$_3$-3′ show considerable variation in $\Delta A_{295}$ depending on the cation present [108]. In our case, the decrease at 295 nm is not due to quadruplex dissociation, but reflects the cation dependence of the nucleic acid absorption at this wavelength.

By MS, only single-stranded oligonucleotide and quadruplex are present in samples, with or without CuTMpyP4. The existence of quadruplex and single-stranded forms of G4 observed in MS and nondenaturing gel electrophoresis is expected because short quadruplexes (with additional bases flanking the guanine tetrads) typically do not exhibit more complex structural heterogeneity [22, 45, 64]. The finding that G10 exists solely in the quadruplex and single-stranded forms when assayed by MS differed from results of native gel electrophoresis in the presence of KCl, which indicated the existence of several multistranded species. Anomalous migration of the intermolecular quadruplex formed by $d(TG_6T)$ has been reported [45], but G6 did not exhibit unusual behavior on native PAGE in our hands. One explanation for the difference between the MS and the PAGE results for G7, G8, G9, and G10 is that gel electrophoresis either promotes formation of or stabilizes oligomeric forms.

As observed for other DNA-binding ligands and G-quadruplexes [11, 17, 22, 24, 39, 42, 43], binding of CuTMpyP4 does not disrupt the G-quadruplex structure. Both MS and native PAGE show that CuTMpyP4 binds to quadruplex and not single-stranded oligonucleotide.

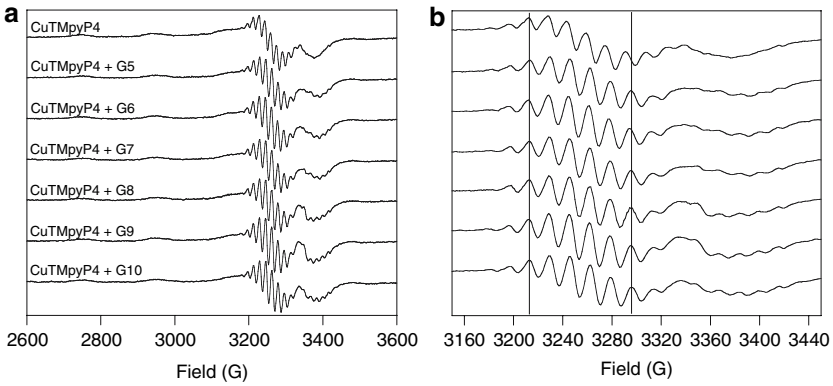


**Fig. 7** X-band electron paramagnetic resonance (EPR) spectra at 20 K of 50 μM CuTMpyP4 in the presence or absence of approximately 100 μM G5, G6, G7, G8, G9, or G10 strand. **a** Full-width spectra. **b** Expanded spectra showing Cu–N superhyperfine peaks with added oligonucleotide. The spectra are in the same order as in **a**. The *vertical lines* in **b** show that the superhyperfine peaks of spectra collected in the presence of oligonucleotide are aligned; the spectrum of CuTMpyP4 alone is different. All spectra are unscaled and the EPR instrumental conditions are in "Materials and methods"

An important question to address is the CuTMpyP4 to quadruplex stoichiometry because of the controversy in the literature regarding free-base porphyrin binding to quadruplexes [24, 43, 48–50]. We applied two different techniques to determine the binding stoichiometry of CuTMpyP4 for quadruplex. The first was high-resolution MS [47, 64, 87–90, 109, 110], a technique that is orthogonal to the second method, continuous-variation analysis [24, 40, 48, 61]. The 2:1 stoichiometry determined by ESI–FTICR–MS is in agreement with previous MS experiments on ethidium bromide, several of its derivatives, and some perylene diimides, which also bind with a stoichiometry of two ligands per quadruplex [47, 88]. In continuous-variation experiments, CuTMpyP4 binding stoichiometry increased as the length of the quadruplex increased. Ligand aggregation is a possible cause of variability in binding stoichiometry [47], but under the conditions used in our experiments, CuTMpyP4 does not aggregate [102, 111–113]. The continuous-variation stoichiometry determinations were at odds with the MS and our other spectroscopic data, which showed no difference as a function of quadruplex length.

The method of continuous variation relies on accurate concentrations of binding partners, a criterion that is difficult to satisfy without knowledge of the quadruplex extinction coefficients [108]. In these experiments, we assumed that the quadruplex extinction coefficient was 4 times that of the single-stranded oligonucleotide extinction coefficient calculated from the nearest-neighbor approximation. The literature for intermolecular quadruplexes indicates there is only a very small hypochromic effect induced by quadruplex formation [46, 114]. For example, the hypochromicity for the intermolecular parallel-stranded quadruplex formed by $d(TG_4)$ is about 5% in 100 mM Tris–HCl at pH 7 and 23 °C [114]. Similarly, Ren and Chaires [46] reported an $A_{260}$ increase of only 0.06 upon melting the intermolecular quadruplex formed by $d(T_2G_{20}T_2)$ in $Na^+$ buffer. Therefore, it is reasonable to use the extinction coefficient of the single-stranded oligonucleotide to calculate that of the corresponding quadruplex. However, we suspected that uncertainty in the quadruplex extinction coefficients for the longer quadruplexes, in particular, could be skewing our ligand binding stoichiometries determined by continuous-variation analysis.

To probe the influence of the quadruplex extinction coefficient on the stoichiometry determined by continuous-variation experiments, the quadruplex extinction coefficient was varied in several repetitions of the continuous-variation experiment. Assuming a 34% lower extinction coefficient for the $(G7)_4$ quadruplex gave a CuTMpyP4 to quadruplex binding stoichiometry of approximately 2:1, whereas assuming a 75% decrease produced Job plots with multiple maxima. Recently, a Job plot with multiple maxima has been reported for ligand binding to an intramolecular quadruplex [115]. In that case, the multiple maxima were interpreted as arising from complexes with increasing ligand stoichiometries (i.e., 1:1, 2:1, 3:1, etc.). When this type of analysis is applied to our Job plot with multiple maxima, the CuTMpyP4 to quadruplex stoichiometries are 0.75:1 and 3:1, which again are not consistent with the MS or our other spectroscopic measurements.

Varying the quadruplex extinction coefficient so that the quadruplex and CuTMpyP4 solutions are equimolar (as described above) is equivalent to conducting continuous-variation experiments with nonequimolar reactant solutions. Use of nonequimolar reactant solutions in continuous-variation experiments to determine binding stoichiometry is documented in the literature [62, 116, 117] and plots generated using this method display maxima that shift as the concentration of one of the reactant solutions is varied [62, 116], just as we observe. Our data therefore indicate that when the quadruplex extinction coefficient of the longer quadruplexes is approximated as 4 times that of the single-stranded oligonucleotide (i.e., no hypochromicity upon formation of the quadruplex), the reactant solution concentrations are not equal, which leads to anomalous ligand binding stoichiometries. These data also lead us to propose that Job plots displaying multiple maxima are an indication that the reactant concentration solutions are not equimolar. Finally, these experiments suggest that differences reported in the literature for the stoichiometry of free-base porphyrin $H_2$TMpyP4 binding to quadruplexes [24, 43, 48, 49] might be explained by errors in the quadruplex concentrations propagated via quadruplex extinction coefficient uncertainty [108].

DNA–porphyrin systems exhibit absorption spectral properties that are associated with a specific type of binding. Intercalation of porphyrins into DNA typically produces a redshift of 15 nm or more and a 35% or more hypochromicity of the porphyrin Soret band in conjunction with a negative induced CD band at the porphyrin Soret band wavelength. External binding results in a redshift of 8 nm or less and either hyperchromicity or hypochromicity of 10% or less of the porphyrin Soret band, and a positive induced CD band in the porphyrin Soret region [52, 113, 118]. For the titrations of CuTMPyP4 with $[d(T_4G_nT_4)_4]$, the Soret band redshifts by 8–8.5 nm and displays hypochromicities of 46–49%. These values are only slightly different from those we measured previously for CuTMpyP4 binding to $(G4)_4$ (redshift, 9 nm; hypochromicity, 50%) [61]. In addition, under conditions where all of the porphyrin is bound, a negative induced CD spectrum is observed. The porphyrin plane has the same orientation with regard to the DNA helical axis whether CuTMpyP4 is end-stacked or intercalated, which means that end-stacking should result in a negative induced CD band. We propose

that the magnitudes of the redshifts and hypochromicities along with the negative induced CD spectrum are signatures of end-stacking in this particular system.

It is tempting to ascribe a redshift of 8–10 nm and a hypochromicity of more than 40% to end-stacking of porphyrins on any intermolecular G-quadruplex. However, the variability in reported values for the free-base porphyrin $H_2$TMpyP4 binding to G-quadruplexes precludes such a generalization. At least four groups have investigated $H_2$TMpyP4 binding to parallel-stranded intermolecular G-quadruplexes [24, 43, 48, 49]. In these papers, the reported Soret band redshifts range from 11 to 18 nm and the hypochromicities range from 40 to 66%. (Note that errors in the quadruplex concentration should have no effect on measurements of the redshift and hypochromicities of the porphyrin Soret band as long as all of the porphyrin is bound.) Part of the explanation for the observed differences could be the identity of the base immediately flanking the guanine-tetrad planes. In sequences in which the porphyrin is proposed to end-stack between thymine and guanine in a quadruplex containing four guanine-tetrad planes, the redshifts are 11–13 nm [24, 43, 48]. On the other hand, a much larger redshift (18 nm) and hypochromicity (66%) are observed when the porphyrin is proposed to bind between adenine and guanine in a sequence containing only three guanine tetrads [49]. The buffer conditions were all slightly different, which also might partly account for the observed range of values. Unfortunately, definitive assignments of redshifts and hypochromicities associated with end-stacking of porphyrins on quadruplexes is still not possible because there is no comprehensive, systematic investigation probing effects exerted by the base adjacent to the guanine-quartet planes on the ligand binding mode and affinity.

To provide further support for our conclusion that the two CuTMpyP4 molecules end-stack on opposite ends of the $[d(T_4G_nT_4)_4]$ quadruplexes, emission and EPR spectra were collected of CuTMpyP4 bound to each of the quadruplexes. Observation of an emission spectrum for CuTMpyP4 typically has been associated with intercalation because intercalation prevents solvent quenching of the CuTMpyP4 excited state [97]. However, we previously showed that CuTMpyP4 bound to the quadruplex formed by $d(T_4G_4T_4)$ exhibits an emission spectrum that is decreased in intensity relative to that observed for CuTMpyP4 intercalated into random-sequence duplex DNA [97]. We observe CuTMpyP4 emission with all of the quadruplexes formed by G5, G6, G7, G8, G9, and G10, indicating that CuTMpyP4 is protected from solvent, but to a lesser degree than if it were intercalated.

There is no correlation between emission intensity of CuTMpyP4 and guanine content of the $d(T_4G_nT_4)$ quadruplexes.

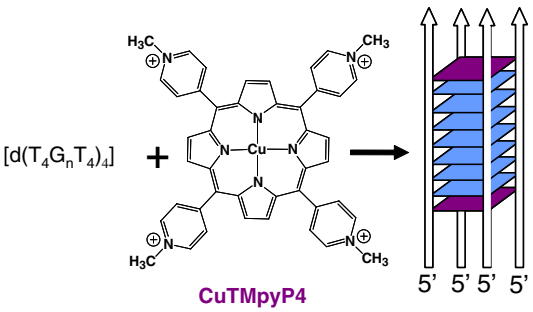


**Scheme 1** Model of *CuTMpyP4* binding to intermolecular parallel-stranded ($n$ = 4–10) G-quadruplexes. *CuTMpyP4* $Cu^{2+}$ derivative of 5,10,15,20-tetrakis(1-methyl-4-pyridyl)-21*H*,23*H*-porphine

Greater emission intensity has been reported for GC-rich DNA than for AT-rich sequences [97]. However, changing the ratio of DNA to copper porphyrin changes the emission intensity, suggesting that the contribution to the overall intensity depends on the distribution of the ligand in different binding sites [120]. In our case, the increase in guanine content ($n$ = 4–10) increases the number of 5′-GG-3′ sites but not the number of 5′-TG-3′ and 5′-GT-3′ end-stacking sites. Our emission data are consistent with the fact that all of the $d(T_4G_nT_4)$ oligonucleotides have the same number of end-stacking sites (two per G-quadruplex) and that the binding stoichiometry is two ligands per quadruplex.

Our EPR spectra also support a model in which the two CuTMpyP4 molecules are not in close proximity (i.e., bound on the same side of the guanine stacks) because CuTMpyP4 bound to quadruplexes does not display an interaction spectrum [98, 102–104]. The EPR data are significant because end-stacking ligands like daunomycin [22] and some perylene diimides [47] bind as aggregates to only one side of the guanine-quartet stacks.

It is reasonable to assume that the $d(T_4G_nT_4)$ quadruplexes used in this work have structures similar to $[d(TG_4T)_4]$ [107]. Given that we obtain a 2:1 binding stoichiometry for CuTMpyP4 bound to the quadruplexes, we propose that CuTMpyP4 end-stacks at each end of the $G_n$-tract, as proposed for binding of other ligands—unrelated to porphyrins—to intermolecular parallel-stranded quadruplexes (Scheme 1) [47, 64, 88, 121, 122].

**Acknowledgments** This work was supported by a grant from Research Corporation (RI1053). Helpful discussions with Daniele Fabris and David H. Stewart are acknowledged.

## References

1. Rankin S, Reszka AP, Huppert J, Zloh M, Parkinson GN, Todd AK, Ladame S, Balasubramanian S, Neidle S (2005) Putative DNA quadruplex formation within the human c-kit oncogene. J Am Chem Soc 127:10584–10589

2. Dexheimer TS, Sun D, Hurley LH (2006) Deconvoluting the structural and drug-recognition complexity of the G-quadruplex-forming region upstream of the bcl-2 P1 promoter. J Am Chem Soc 128:5404–5415
3. De Armond R, Wood S, Sun D, Hurley LH, Ebbinghaus SW (2005) Evidence for the presence of a guanine quadruplex forming region within a polypurine tract of the hypoxia inducible factor 1alpha promoter. Biochemistry 44:16341–16350
4. Siddiqui-Jain A, Grand CL, Bearss DJ, Hurley LH (2002) Direct evidence for a G-quadruplex in a promoter region and its targeting with a small molecule to repress c-MYC transcription. Proc Natl Acad Sci USA 99:11593–11598
5. Arthanari H, Bolton PH (2001) Functional and dysfunctional roles of quadruplex DNA in cells. Chem Biol 8:221–230
6. Paeschke K, Simonsson T, Postberg J, Rhodes D, Lipps HJ (2005) Telomere end-binding proteins control the formation of G-quadruplex DNA structures in vivo. Nat Struct Mol Biol 12:847–854
7. Levens D, Duncan RC, Tomonaga T, Michelotti GA, Collins I, Davis-Smyth T, Zheng T, Michelotti EF (1997) DNA conformation, topology, and the regulation of c-myc expression. Curr Top Microbiol Immunol 224:33–46
8. Darnell JC, Jensen KB, Jin P, Brown V, Warren ST, Darnell RB (2001) Fragile X mental retardation protein targets G quartet mRNAs important for neuronal function. Cell 107:489–499
9. Mergny J-L, Mailliet P, Lavelle F, Riou J-F, Lauoi A, Hélène C (1999) The development of telomerase inhibitors: the G-quartet approach. Anticancer Drug Des 14:327–339
10. Izbicka E, Wheelhouse RT, Raymond E, Davidson KK, Lawrence RA, Sun D, Windle BE, Hurley LH, Von Hoff DD (1999) Effects of cationic porphyrins as G-quadruplex interactive agents in human tumor cells. Cancer Res 59:639–644
11. Read MA, Neidle S (2000) Structural characterization of a guanine-quadruplex ligand complex. Biochemistry 39:13422–13432
12. Neidle S, Parkinson G (2002) Telomere maintenance as a target for anticancer drug discovery. Nat Rev Drug Discov 1:383–393
13. Parkinson GN, Lee MPH, Neidle S (2002) Crystal structure of parallel quadruplexes from human telomeric DNA. Nature 417:876–880
14. Han H, Langley DR, Rangan A, Hurley LH (2001) Selective interactions of cationic porphyrins with G-quadruplex structures. J Am Chem Soc 123:8902–8913
15. Sun D, Thompson B, Cathers BE, Salazar M, Kerwin SM, Trent JO, Jenkins TC, Neidle S, Hurley LH (1997) Inhibition of human telomerase by a G-quadruplex-interactive compound. J Med Chem 40:2113–2116
16. Han H, Bennett RJ, Hurley LH (2000) Inhibition of unwinding of G-quadruplex structures by Sgs1 helicase in the presence of N,N′-bis[2-(1-piperidino)ethyl]3,4,9,10-perylenetetracarboxylic diimide, a G-quadruplex-interactive ligand. Biochemistry 39:9311–9316
17. Haider SM, Parkinson GN, Neidle S (2003) Structure of a G-quadruplex–ligand complex. J Mol Biol 326:117–125
18. Shi D, Wheelhouse RT, Sun D, Hurley LH (2001) Quadruplex-interactive agents as telomerase inhibitors: synthesis of porphyrins and structure–activity relationships for the inhibition of telomerase. J Med Chem 44:4509–4523
19. Nakatani K, Hagihara S, Sando S, Sakamoto S, Yamaguchi K, Maesawa C, Saito I (2003) Induction of a remarkable conformational change in a human telomeric sequence by the binding of naphthyridine dimer: inhibition of the elongation of a telomeric repeat by telomerase. J Am Chem Soc 125:662–666
20. Grand CL, Han H, Munoz RM, Weitman S, Von Hoff DD, Hurley LH, Bearss DJ (2002) The cationic porphyrin TMPyP4 down-regulates c-MYC and human telomerase reverse transcriptase expression and inhibits tumor growth in vivo. Mol Cancer Ther 1:565–573
21. Fedoroff OY, Salazar M, Han H, Chemeris VV, Kerwin SM, Hurley LH (1998) NMR-based model of a telomerase-inhibiting compound bound to G-quadruplex DNA. Biochemistry 37:12367–12374
22. Clark GR, Pytel PD, Squire CJ, Neidle S (2003) Structure of the first parallel DNA quadruplex–drug complex. J Am Chem Soc 125:4066–4067
23. Vialas C, Pratviel G, Meunier B (2000) Oxidative damage generated by an oxo-metalloporphyrin onto the human telomeric sequence. Biochemistry 39:9514–9522
24. Haq I, Trent JO, Chowdhry BZ, Jenkins TC (1999) Intercalative G-tetraplex stabilization of telomeric DNA by a cationic porphyrin. J Am Chem Soc 121:1768–1779
25. Granotier C, Pennarun G, Riou L, Hoffschir F, Gauthier LR, De Cian A, Gomez D, Mandine E, Riou JF, Mergny JL, Mailliet P, Dutrillaux B, Boussin FD (2005) Preferential binding of a G-quadruplex ligand to human chromosome ends. Nucleic Acids Res 33:4182–4190
26. Barbieri CM, Srinivasan AR, Rzuczek SG, Rice JE, LaVoie EJ, Pilch DS (2007) Defining the mode, energetics, and specificity with which a macrocyclic hexazole binds to human telomeric G-quadruplex DNA. Nucleic Acids Res 35:3272–3286
27. He F, Tang Y, Wang S, Li Y, Zhu D (2005) Fluorescent amplifying recognition for DNA G-quadruplex folding with a cationic conjugated polymer: a platform for homogeneous potassium detection. J Am Chem Soc 127:12343–12346
28. Halder K, Chowdhury S (2005) Kinetic resolution of bimolecular hybridization versus intramolecular folding in nucleic acids by surface plasmon resonance: application to G-quadruplex/duplex competition in human c-myc promoter. Nucleic Acids Res 33:4466–4474
29. Zeng ZX, Zhao Y, Hao YH, Tan Z (2005) Tetraplex formation of surface-immobilized human telomere sequence probed by surface plasmon resonance using single-stranded DNA binding protein. J Mol Recognit 18:267–271
30. Zhao Y, Kan ZY, Zeng ZX, Hao YH, Chen H, Tan Z (2004) Determining the folding and unfolding rate constants of nucleic acids by biosensor. Application to telomere G-quadruplex. J Am Chem Soc 126:13255–13264
31. Whitney AM, Ladame S, Balasubramanian S (2004) Templated ligand assembly by using G-quadruplex DNA and dynamic covalent chemistry. Angew Chem Int Ed Engl 43:1143–1146
32. Miyoshi D, Nakao A, Sugimoto N (2003) Structural transition from antiparallel to parallel G-quadruplex of $d(G_4T_4G_4)$ induced by $Ca^{2+}$. Nucleic Acids Res 31:1156–1163
33. Alberti P, Bourdoncle A, Sacca B, Lacroix L, Mergny J-L (2006) DNA nanomachines and nanostructures involving quadruplexes. Org Biomol Chem 4:3383–3391
34. Bourdoncle A, Torres AE, Gosse C, Lacroix L, Vekhoff P, Le Saux T, Jullien L, Mergny J-L (2006) Quadruplex-based molecular Beacons as tunable DNA probes. J Am Chem Soc 128:11094–11105
35. Kotlyar AB, Borovok N, Molotsky T, Cohen H, Shapir E, Porath D (2005) Long monomolecular guanine-based nanowires. Adv Mater 17:1901–1905
36. Marsh TC, Vesenka J, Henderson E (1995) A new DNA nanostructure, the G-wire, imaged by scanning probe microscopy. Nucleic Acids Res 23:696–700
37. Miyoshi D, Karimata H, Wang Z-M, Koumoto K, Sugimoto N (2007) Artificial G-wire switches with 2,2′-bipyridine units responsive to divalent metal ions. J Am Chem Soc 129:5919–5925
38. Kim M-Y, Duan W, Gleason-Guzman M, Hurley LH (2003) Design, synthesis, and biological evaluation of a series of

fluoroquinoanthroxazines with contrasting dual mechanisms of action against topoisomerase II and G-quadruplexes. J Med Chem 46:571–583
39. Han FX, Wheelhouse RT, Hurley LH (1999) Interactions of TMPyP4 and TMPyP2 with quadruplex DNA. Structural basis for the differential effects on telomerase inhibition. J Am Chem Soc 121:3561–3570
40. Wheelhouse RT, Sun D, Han H, Han FX, Hurley LH (1998) Cationic porphyrins as telomerase inhibitors: the interaction of tetra-(*N*-methyl-4-pyridyl)porphine with quadruplex DNA. J Am Chem Soc 120:3261–3262
41. Kim M-Y, Vankayalapati H, Shin-ya K, Wierzba K, Hurley LH (2002) Telemostatin, a potent telomerase inhibitor that interacts quite specifically with the human telomeric intramolecular G-quadruplex. J Am Chem Soc 124:2098–2099
42. Read MA, Wood AA, Harrison JR, Gowan SM, Kelland LR, Dosanjh HS, Neidle S (1999) Molecular modeling studies on G-quadruplex complexes of telomerase inhibitors: structure–activity relationships. J Med Chem 42:4538–4546
43. Anantha NV, Azam N, Sheardy RD (1998) Porphyrin binding to quadruplexed T4G4. Biochemistry 37:2709–2714
44. Arimondo PB, Riou J-F, Mergny J-L, Tazi J, Sun J-S, Garestier T, Helene C (2000) Interaction of human DNA topoisomerase I with G-quartet structures. Nucleic Acids Res 28:4832–4838
45. Mergny JL, De Cian A, Ghelab A, Sacca B, Lacroix L (2005) Kinetics of tetramolecular quadruplexes. Nucleic Acids Res 33:81–94
46. Ren J, Chaires JB (1999) Sequence and structural selectivity of nucleic acid binding ligands. Biochemistry 38:16067–16075
47. Mazzitelli CL, Brodbelt JS, Kern JT, Rodriguez M, Kerwin SM (2006) Evaluation of binding of perylene diimide and benz-annulated perylene diimide ligands to DNA by electrospray ionization mass spectrometry. J Am Soc Mass Spectrom 17:593–604
48. Wei C, Jia G, Yuan J, Feng Z, Li C (2006) A spectroscopic study on the interactions of porphyrin with G-quadruplex DNAs. Biochemistry 45:6681–6691
49. Mita H, Ohyama T, Tanaka Y, Yamamoto Y (2006) Formation of a complex of 5,10,15:20-tetrakis(*N*-methylpyridinium-4-yl)21H, 23H-porphyrin with G-quadruplex DNA. Biochemistry 45:6765–6772
50. Phan AT, Kuryavyi V, Gaw HY, Patel DJ (2005) Small molecule interaction with a five-guanine tract G-quadruplex structure from the human MYC promoter. Nat Chem Biol 1:167–173
51. Reed JE, Arnal AA, Neidle S, Vilar R (2006) Stabilization of G-quadruplex DNA and inhibition of telomerase activity by square-planar nickel(II) complexes. J Am Chem Soc 128:5992–5993
52. Pasternack RF, Gibbs EJ, Villafranca JJ (1983) Interactions of porphyrins with nucleic acids. Biochemistry 22:5409–5417
53. Borer PN (1975) Optical properties of nucleic acids, absorption, and circular dichroism spectra. In: Fasman G (ed) Handbook of biochemistry and molecular biology. CRC, Cleveland, p 589
54. Merkina EE, Fox KR (2005) Kinetic stability of intermolecular DNA quadruplexes. Biophys J 89:365–373
55. Sen D, Gilbert W (1990) A sodium–potassium switch in the formation of four-stranded G4-DNA. Nature 344:410–414
56. Lu M, Guo Q, Kallenbach NR (1992) Structure and stability of sodium and potassium complexes of dT4G4 and dT4G4T. Biochemistry 31:2455–2459
57. Hardin CC, Perry AG, White K (2001) Thermodynamic and kinetic characterization of the dissociation and assembly of quadruplex nucleic acids. Biopolymers 56:147–194
58. Lyonnais S, Hounsou C, Teulade-Fichou MP, Jeusset J, Le Cam E, Mirambeau G (2002) G-quartets assemly within a G-rich DNA flap. A possible event at the center of the HIV-1 genome. Nucleic Acids Res 30:5276–5283
59. Plum GE (2000) Current protocols in nucleic acid chemistry. Wiley, New York, p 7.3.1
60. Szalai VA, Thorp HH (2000) Electron transfer in tetrads: adjacent guanines are not hole traps in G quartets. J Am Chem Soc 122:4524–4525
61. Keating LR, Szalai VA (2004) Parallel-stranded guanine quadruplex interactions with a copper cationic porphyrin. Biochemistry 43:15891–15900
62. Ramanathan PS, Venkateswarlu C, Walvekar AP (1975) On the experimental approach to continuous variation method in equimolar solutions. Indian J Chem 13:739–741
63. Rosu F, Gabelica V, Houssier C, Colson P, Pauw ED (2002) Triplex and quadruplex DNA structures studied by electrospray mass spectrometry. Rapid Commun Mass Spectrom 16:1729–1736
64. David WM, Brodbelt J, Kerwin SM, Thomas PW (2002) Investigation of quadruplex oligonucleotide–drug interactions by electrospray ionization mass spectrometry. Anal Chem 74:2029–2033
65. Loo JA (1997) Studying noncovalent protein complexes by electrospray ionization mass spectrometry. Mass Spectrom Rev 16:1–23
66. Hagan NA, Fabris D (2003) A direct mass spectrometric determination of the stoichiometry and binding affinity of the complexes between HIV-1 nucleocapsid protein and RNA stem-loops hairpins of the HIV-1 Ψ-recognition element. Biochemistry 42:10736–10745
67. Keniry MA (2001) Quadruplex structures in nucleic acids. Biopolymers 56:123–146
68. Kowalczykowski S, Leland S, Lonberg N, Newport J, McSwiggen J, von Hippel PH (1986) Cooperative and noncooperative binding of protein ligands to nucleic acid lattices: experimental approaches to the determination of thermodynamic parameters. Biochemistry 25:1226–1240
69. Klotz IM (1997) Ligand–receptor energetics: a guide for the perplexed. Wiley, New York
70. McGhee JD, von Hippel PH (1974) Theoretical aspects of DNA–protein interactions: co-operative and non-co-operative binding of large ligands to a one-dimensional homogeneous lattice. J Mol Biol 86:469–489
71. Aleksandrov ML, Gall LN, Krasnov VN, Nikolaev VI, Pavlenko VA, Shkurov VA (1984) Exraction of ions from solutions under atmospheric pressure: a method of mass spectrometric analysis of bioorganic compounds. Dokl Akad Nauk 277:379–383
72. Yamashita M, Fenn JB (1984) Electrospray ion source. Another variation on the free-jet theme. J Phys Chem 88:4671–4675
73. Hofstadler SA, Griffey RH (2001) Analysis of noncovalent complexes of DNA and RNA by mass spectrometry. Chem Rev 101:377–390
74. Hofstadler SA, Sannes-Lowery KA, Hannis JC (2005) Analysis of nucleic acids by FTICR MS. Mass Spectrom Rev 24:265–285
75. Beck JL, Colgrave ML, Ralph SF, Sheil MM (2001) Electrospray ionization mass spectrometry of oligonucleotide complexes with drugs, metals and proteins. Mass Spectrom Rev 2001:61–87
76. Kapur A, Beck JL, Sheil MM (1999) Observation of daunomycin and nogalamycin complexes with duplex DNA using electrospray ionization mass spectrometry. Rapid Commun Mass Spectrom 13:2489–2497
77. Gabelica V, De Pauw E, Rosu F (1999) Interaction between antitumor drugs and a double-stranded oligonucleotide studied by electrospray ionization mass spectrometry. J Mass Spectrom 34:1328–1337

78. Sannes-Lowery KA, Mei H-Y, Loo JA (1999) Studying aminoglycoside antibiotic binding to HIV-1 TAR RNA by electrospray ionization mass spectrometry. Int J Mass Spectrom Ion Processes 193:115–122
79. Hofstadler SA, Sannes-Lowery KA, Crooke ST, Ecker DJ, Sasmor H, Manalili G, Griffey RH (1999) Multiplexed screening of neutral mass-tagged RNA targets against ligand libraries with electrospray ionization FTICR MS: a paradigm for high-throughput affinity screening. Anal Chem 71:3426–3440
80. Turner KB, Hagan NA, Fabris D (2006) Inhibitory effects of archetypical nucleic acid ligands on the interactions of HIV-1 nucleocapsid protein with elements of Ψ-RNA. Nucleic Acids Res 34:1305–1316
81. Wan KX, Shibue T, Gross ML (2000) Non-covalent complexes between DNA-binding drugs and double-stranded oligodeoxynucleotides: a study by ESI ion-trap mass spectrometry. J Am Chem Soc 122:300–307
82. Griffey RH, Hofstadler SA, Sannes-Lowery KA, Ecker DJ, Crooke ST (1999) Determinants of aminoglycoside-binding specificity for rRNA by using mass spectrometry. Proc Natl Acad Sci USA 96:10129–10133
83. Sannes-Lowery KA, Griffey RH, Hofstadler SA (2000) Measuring dissociation constants of RNA and aminoglycoside antibiotics by electrospray ionization mass spectrometry. Anal Biochem 280:264–271
84. Rosu F, Gabelica V, Houssier C, De Pauw E (2002) Determination of affinity, stoichiometry and sequence selectivity of minor groove binder complexes with double-stranded oligodeoxynucleotides by electrospray ionization mass spectrometry. Nucleic Acids Res 30:e82
85. Gooding KB, Higgs R, Hodge B, Stauffer E, Heinz B, McKnight K, Phipps K, Shapiro M, Winkler M, Ng WL, Julian RK (2004) High throughput screening of library compounds against an oligonucleotide substructure of an RNA target. J Am Soc Mass Spectrom 15:884–892
86. David WM, Brodbelt JS, Kerwin SM, Thomas PW (2002) Investigation of quadruplex oligonucleotide–drug interaction by electrospray ionization mass spectrometry. Anal Chem 74:2029–2033
87. Carrasco C, Rosu F, Gabelica V, Houssier C, De Pauw E, Garbay-Jaureguiberry C, Roques B, Wilson WD, Chaires JB, Waring MJ, Bailly C (2002) Tight binding of the antitumor drug ditercalinium to quadruplex DNA. Chembiochem 3:1235–1241
88. Rosu F, De Pauw E, Guittat L, Alberti P, Lacroix L, Mailliet P, Riou JF, Mergny JL (2003) Selective interaction of ethidium derivatives with quadruplexes: an equilibrium dialysis and electrospray ionization mass spectrometry analysis. Biochemistry 42:10361–10371
89. Rosu F, Gabelica V, Shin-ya K, De Pauw E (2003) Telomestatin-induced stabilization of the human telomeric DNA quadruplex monitored by electrospray mass spectrometry. Chem Commun 2702–2703
90. Guittat L, De Cian A, Rosu F, Gabelica V, De Pauw E, Delfourne E, Mergny JL (2005) Ascididemin and meridine stabilise G-quadruplexes and inhibit telomerase in vitro. Biochim Biophys Acta 1724:375–384
91. Hendrickson CL, Emmett MR, Marshall AG (1999) Electrospray ionization Fourier transform ion cyclotron resonance mass spectrometry. Annu Rev Phys Chem 50:517–536
92. Comisarow MB, Marshall AG (1974) Fourier transform ion cyclotron resonance. Chem Phys Lett 25:282–283
93. Griffey RH, Sannes-Lowery KA, Drader JJ, Mohan V, Swayze EE, Hofstadler SA (2000) Characterization of low-affinity complexes between RNA and small molecules using electrospray ionization mass spectrometry. J Am Chem Soc 122: 9933–9938
94. Job P (1928) Recherches sur la formation de complexes mineraux en solutions, et sur leur stabilite. Ann Chim 9:113–134
95. Musier KM, Hammes GG (1988) Assessment of the number of nucleotide binding sites on chloroplast coupling factor 1 by the continuous variation method. Biochemistry 27:7015–7020
96. Huang CY (1982) Determination of binding stoichiometry by the continuous variation method: the Job plot. Methods Enzymol 87:509–525
97. Hudson BP, Sou J, Berger DJ, McMillin DR (1992) Luminescence studies of the intercalation of Cu(TMpyP4) into DNA. J Am Chem Soc 114:8997–9002
98. Blumberg WE, Peisach J (1965) An electron spin resonance study of copper uroporphyrin III and other touraco feather components. J Biol Chem 240:870–876
99. Subramanian J (1975) Electron paramagnetic resonance spectroscopy of porphyrins and metalloporphyrins. In: Smith KM (ed) Porphyrins and metalloporphyrins. Elsevier, Amsterdam, pp 555–589
100. Dougherty G, Pilbrow JR, Skorobogaty A, Smith TD (1985) Electron spin resonance spectroscopic and spectrophotometric investigation of the binding of tetracationic porphryins and porphyrazines with calf thymus DNA. J Chem Soc Far Trans 81:1739–1759
101. Dougherty G (1988) Intercalation of tetracationic metalloporphyrins and related compounds into DNA. J Inorg Biochem 34:95–103
102. Dougherty G, Pasternack RF (1992) Aggregation of copper(II) derivatives of meso-substituted porphyrins in frozen aqueous media. Inorg Chim Acta 195:95–100
103. Skorobogaty A, Smith TD, Dougherty G, Pilbrow JR (1985) Synthesis and physico-chemical properties of cationic derivatives of phthalocyaninatocopper(II). J Chem Soc Dalton Trans 651–658
104. Eaton SS, Eaton GR, Chang CK (1985) Synthesis and geometry determination of cofacial diporphyrins. EPR spectroscopy of dicopper diporphyrins in frozen solution. J Am Chem Soc 107:3177–3184
105. Gupta G, Garcia AE, Guo Q, Lu M, Kallenbach NR (1993) Structure of a parallel-stranded tetramer of the oxytricha telomeric DNA sequence of dT4G4. Biochemistry 32:7098–7103
106. Laughlan G, Murchie AIH, Norman DG, Moore MH, Moody PCE, Lilley DMJ, Luisi B (1994) The high-resolution crystal structure of a parallel-stranded guanine tetraplex. Science 265:520–524
107. Phillips K, Dauter Z, Murchie AIH, Lilley DMJ Luisi B (1997) The crystal structure of a parallel-stranded guanine tetraplex at 0.95 Å resolution. J Mol Biol 273:171–182
108. Mergny JL, Li J, Lacroix L, Amrane S, Chaires JB (2005) Thermal difference spectra: a specific signature for nucleic acid structures. Nucleic Acids Res 33:e138
109. Guittat L, Alberti P, Rosu F, Van Miert S, Thetiot E, Pieters L, Gabelica V, De Pauw E, Ottaviani A, Riou JF, Mergny JL (2003) Interactions of cryptolepine and neocryptolepine with unusual DNA structures. Biochimie 85:535–547
110. Pothukuchy A, Mazzitelli CL, Rodriguez ML, Tuesuwan B, Salazar M, Brodbelt JS, Kerwin SM (2005) Duplex and quadruplex DNA binding and photocleavage by trioxatriangulenium ion. Biochemistry 44:2163–2172
111. Pasternack RF, Francesconi L, Raff J, Spiro E (1973) Aggregation of nickel(II), copper(II), and zinc(II) derivatives of water-soluble porphyrins. Inorg Chem 12:2606–2611
112. Pasternack RF, Huber PR, Boyd PDW Engasser G, Francesconi L, Gibbs EJ, Fasella P, Venturo GC, Hinds Ld (1972) On the aggregation of meso-substituted water-soluble porphryins. J Am Chem Soc 94:4511–4517

113. Pasternack RF, Gibbs EJ, Gaudemer A, Antebi A, Bassner S, DePoy L, Turner DH, Williams A, Laplace F, Lansard MH, Merienne C, Perree-Fauvet M (1985) Molecular complexes of nucleosides and nucleotides with a monomeric cationic porphyrin and some of its metal derivatives. J Am Chem Soc 107:8179–8186
114. Hardin CC, Corregan MJ, Lieberman DV, Brown BAI (1997) Allosteric interactions between DNA strands and monovalent cations in DNA quadruplex assembly: thermodynamic evidence for three linked association pathways. Biochemistry 36:15428–15450
115. Freyer MW, Buscaglia R, Kaplan K, Cashman D, Hurley LH, Lewis EA (2007) Biophysical studies of the c-MYC NHE III1 promoter: model quadruplex interactions with a cationic porphyrin. Biophys J 92:2007–2015
116. Walvekar AP, Ramanathan PS (1981) Application of continuous variation method in nonequimolar solutions to systems involving stable stepwise complexes. Indian J Chem 20A:154–162
117. Douillard R (1974) Etude theorique de la determination des coefficients stoichiometriques des reactions chimiques: extension de la methode dea variations continues au cas ou les solutions-meres ne sont pas equimoleculaires. C R Acad Sci Paris Ser C 278:1441–1444
118. Pasternack RF, Gibbs EJ (1989) Interaction of porphyrins and metalloporphyrins with nucleic acids. In: Tullius T (ed) Metal–DNA chemistry. American Chemical Society, Washington, pp 59–73
119. McMillin DR, Shelton AH, Bejune SA, Fanwick PE, Wall RK (2005) Understanding binding interactions of cationic porphyrins with B-form DNA. Coord Chem Rev 249:1451–1459
120. Eggleston MK, Crites DK, McMillin DR (1998) Studies of the base-dependent binding of Cu(T4) to DNA hairpins ($H_2$T4 = *meso*-tetrakis(4-(*N*-methylpyridiniumyl)porphyrin). J Phys Chem A 102:5506–5511
121. Kerwin SM, Chen G, Kern JT, Thomas PW (2002) Perylene diimide G-quadruplex DNA binding selectivity is mediated by ligand aggregation. Bioorg Med Chem Lett 12:447–450
122. De Cian A, Mergny J-L (2007) Quadruplex ligands may act as molecular chaperones for tetramolecular quadruplex formation. Nucleic Acids Res 35:2483–2493